LOAD-DEFLECTION RELATIONS OF T-SECTION RAILS UNDER LATERAL LOADS

Youshuo Song, Zhonghua Yu

Zhejiang University, Institute of Modern Manufacturing Engineering, Hangzhou, China
e-mail: caq_221@zju.edu.cn

This paper studies the load-deflection relations of T-section rails under lateral loads based on elastic-plastic theory. A linear-hardening model and an elastic-plastic power-exponent hardening model of the material are adopted in this study. The analytical expressions for the load-deflection relations in the loading process are given. Compared with the experimental results, it is found that the load-deflection curves calculated with the elastic-plastic power-exponent hardening model are closer to the experimental results than those with the linear-hardening model.

Key words: T-section rail, load-deflection relations, lateral loads, linear-hardening model

1. Introduction

Straightening is an important process in the production route of a T-section rail (Biempica *et al.*, 2009; Volebov *et al.*, 1994). In practice, the most common method for T-section rail straightening is the three points reverse bending based on handwork and the worker's experience. So the quality and efficiency is hard to guarantee. To meet higher production requirements, an automatic rail straightening machine is to be developed, and the load-deflection model of the bending process is suitable to be used on the straightening control (Li *et al.*, 2004).

Deflections of sandwich beams subject to concentrated or localized loads have been studied, and it is sufficient to accurately predict the vertical displacements in the face sheets of a sandwich beam (Shen *et al.*, 2004; Sokolinsky *et al.*, 2003). Also, a number of studies have been proposed in order to investigate the load-deflection relationships of concrete beams reinforced with FRP bars (Ou *et al.*, 2004; Masmoudi *et al.*, 1998). Tsai and Kan (2008) studied the load-deflection model of the uniformly loaded rectangular cross-section cantilever beam. According to Tsai *et al.* (2009), various loading scenarios can result in different deflection profiles, albeit with the same tip deflection.

The material hardening parameters can be determined by comparing load–displacement curves from FE simulations with those from tests in the cyclic three-point bending test (Omerspahic *et al.*, 2006; Eggertsen and Mattiasson, 1998). Studies were also conducted on the load-deflection relations of some components that have regular cross sections such as shafts, pipes and the rectangular section part (Li and Xiong, 2007; Katoh and Urata, 1993). However, because of its complicated cross section with large size, few investigations have be done on the load-deflection relations for the T-section rail straightening process.

In this paper, the load-deflection relations of T-section rails under lateral loads are studied based on elastic-plastic theory. The linear hardening model and the elastic-plastic power-exponent hardening model are used for the analysis. Two experiments are also carried out to verify the accuracy of the model. It will be applied on the automatic T-section rail straightening machine.

2.   Establishment of the load-deflection relations

2.1.   Elastic deformation stage

The following assumptions are accepted in this study:
- The plane section assumption and uniaxial stress assumption are reasonable.
- The Bauschinger effect and the reverse plastic deformation during unloading are neglected.
- Compared with the distance between the two support points, the deflection of the rail is small.

The T shaped cross section of the rail is shown in Fig. 1. In this work, analysis is carried out on the lateral bending deformation of the rail.
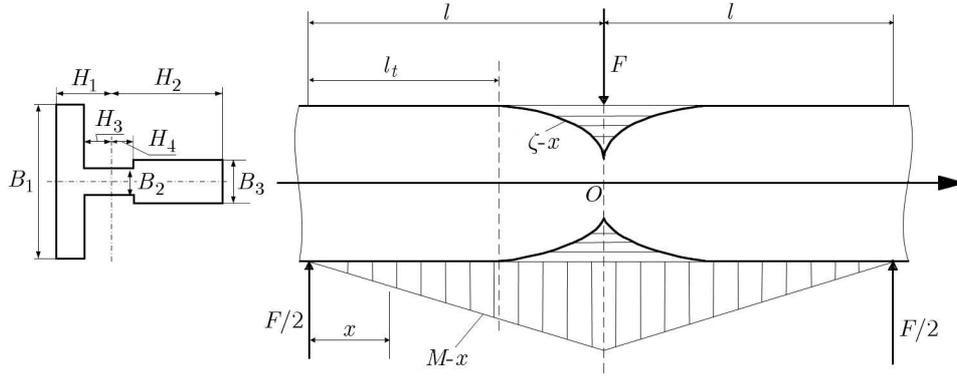

Fig. 1. Plastic region and bending moment distribution

At the elastic deformation stage, the relationship between the deflection and loading force can be written according to material mechanics

$$\delta = \frac{l^3}{6EI}F \qquad F \leqslant \frac{2M_t}{l} \tag{2.1}$$

where

$$I = \frac{(H_1 - H_3)B_1^3 + (H_3 + H_4)B_2^3 + (H_2 - H_4B_3^3)}{12}$$

is the inertia moment against neutral axis of the cross-section, and $2l$ is the distance between the two support points, and E is Young's modulus.

And the maximum elastic bending moment M_t can be written as

$$M_t = \frac{\sigma_s}{6B_1}[(H_1 - H_3)B_1^3 + (H_3 + H_4)B_2^3 + (H_2 - H_4)B_3^3] \tag{2.2}$$

where σ_s is the yield stress of the material.

2.2.   Elastic-plastic deformation stage

2.2.1.   Linear-hardening model

At this stage, plastic deformation occurs from the outer fiber in the material and the dashed area in Fig. 1 is the plastic region (Li *et al.*, 2004).

In the linear-hardening case, the stress-strain relation for the rail material is as follows

$$\sigma = \begin{cases} E\varepsilon & \text{for} \quad \varepsilon \leqslant \varepsilon_s \\ \sigma_s + E_P(\varepsilon - \varepsilon_s) & \text{for} \quad \varepsilon \geqslant \varepsilon_s \end{cases} \tag{2.3}$$

where ε_s is the strain at the yield point, E_p the linear hardening modulus, σ the true stress and ε the true strain.

Figure 2 shows the stress distribution through the rail section after bending, so that (Johnson and Yu, 1981)

$$\sigma = \begin{cases} \sigma_s \dfrac{z}{z_s} & \text{for} \quad 0 \leqslant z \leqslant z_s \\[2mm] \sigma_s \left[1 + \lambda\left(\dfrac{z}{z_s} - 1\right)\right] & \text{for} \quad z_s \leqslant z \leqslant \dfrac{B_1}{2} \end{cases} \tag{2.4}$$
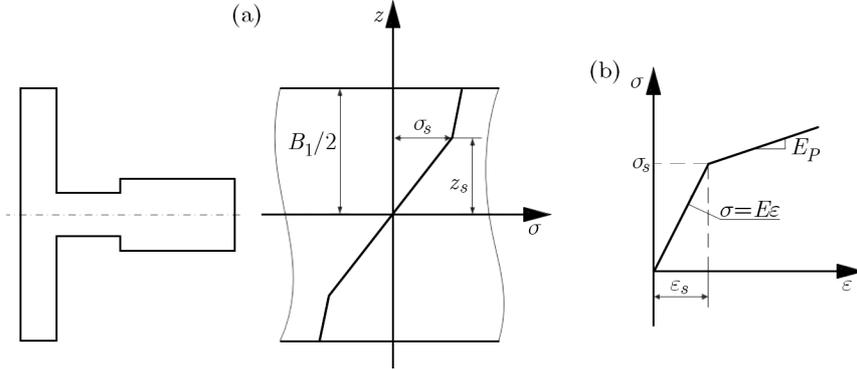
where $\lambda = E_P/E$.

Fig. 2. The stress distribution through the rail section after bending: (a) stress distribution after bending, (b) stress-strain curve of linear hardening material

The width of the rail foot is much larger than that of the rail web and head, so generally no fibers of the rail web and head are strained beyond the yield limit during deformation. Then, for the force equilibrium across the section

$$M_x = 2 \int_0^{z_s} z\frac{z}{z_s}\sigma_s(H_1 - H_3)\, dz + 2 \int_0^{\frac{B_2}{2}} z\frac{z}{z_s}\sigma_s(H_3 + H_4)\, dz + 2 \int_0^{\frac{B_3}{2}} z\frac{z}{z_s}\sigma_s(H_2 - H_4)\, dz$$
$$+ 2 \int_{z_s}^{\frac{B_1}{2}} z\left[1 + \lambda\left(\frac{z}{z_s} - 1\right)\right]\sigma_s(H_1 - H_3)\, dz \tag{2.5}$$

where M_x is the bending moment imposed on the rail section and z_s is the distance between fibers which are just at yield and the neutral axis.

Equations (2.5) and (2.2) reduce to the following equation

$$\frac{M_x}{M_t} = \frac{1}{\xi}\left[1 + \frac{1}{2}\frac{(\lambda - 1)(H_1 - H_3)B_1^3(\xi^3 - 3\xi + 2)}{(H_1 - H_3)B_1^3 + (H_3 + H_4)B_2^3 + (H_2 - H_4)B_3^3}\right] \tag{2.6}$$

where $\xi = z_s/(B_1/2)$ is the relative elastic zone ratio and $\xi \geqslant B_3/B_1$.

And M_x can also be written as

$$M_x = \frac{F}{2}x \tag{2.7}$$

Let $\overline{C_\Sigma}$ be the relative change of total curvature of the rail, then based on the plane supposition of elastic-plastic bending and elastic mechanics (Wu *et al.*, 2000)

$$\xi = \frac{1}{\overline{C_\Sigma}} = \frac{C_t}{C_\Sigma} \tag{2.8}$$

where $C_t = M_t/(EI)$.

Then, from equations (2.6)-(2.8), the relation between C_Σ and x can be obtained

$$\frac{Fx}{2M_t} = \frac{C_\Sigma}{C_t} + \frac{1}{2} \frac{(\lambda-1)(H_1-H_3)B_1^3 \left[\left(\frac{C_\Sigma}{C_t}\right)^{-2} + 2\frac{C_\Sigma}{C_t} - 3\right]}{(H_1-H_3)B_1^3 + (H_3+H_4)B_2^3 + (H_2-H_4)B_3^3} \tag{2.9}$$
$$\frac{2M_t}{F} \leqslant x \leqslant l$$

And the loading stroke at the middle point, i.e. deflection, can be obtained (Chui, 1994)

$$\delta_\Sigma = \frac{Fl_t^3}{6EI} + \sum_{i=1}^n x_i C_{\Sigma xi} \Delta x \qquad\qquad F \geqslant \frac{2M_t}{l} \tag{2.10}$$

where

$$l_t = \frac{2M_t}{F} \qquad\qquad \Delta x = \frac{l-l_t}{n} \qquad\qquad x_i = l_t + i\Delta x$$

So, combining equations (2.9) and (2.10), if the loading force F is given, δ_Σ can be calculated under the linear-hardening model.

2.2.2. *Elastic-plastic power-exponent hardening model*

The elastic-plastic power-exponent hardening model is as follows (Johnson and Yu, 1981)

$$\sigma = \begin{cases} E\varepsilon & \text{for} \quad \varepsilon \leqslant \varepsilon_s \\ E\varepsilon - K(\varepsilon-\varepsilon_s)^n & \text{for} \quad \varepsilon \geqslant \varepsilon_s \end{cases} \tag{2.11}$$

where K, and $n \geqslant 1$ are the hardening coefficient and the hardening exponent, respectively.

Figure 3 shows the stress distribution through the rail section after bending under the elastic-plastic power-exponent hardening model.

Similar to equation (2.4), it can be proven that (Johnson and Yu, 1981)

$$\sigma = \begin{cases} \sigma_s \dfrac{z}{z_s} & \text{for} \quad 0 \leqslant z \leqslant z_s \\ \sigma_s \dfrac{z}{z_s} - K'\left(\dfrac{z}{z_s}-1\right)^n & \text{for} \quad z_s \leqslant z \leqslant \dfrac{B_1}{2} \end{cases} \tag{2.12}$$
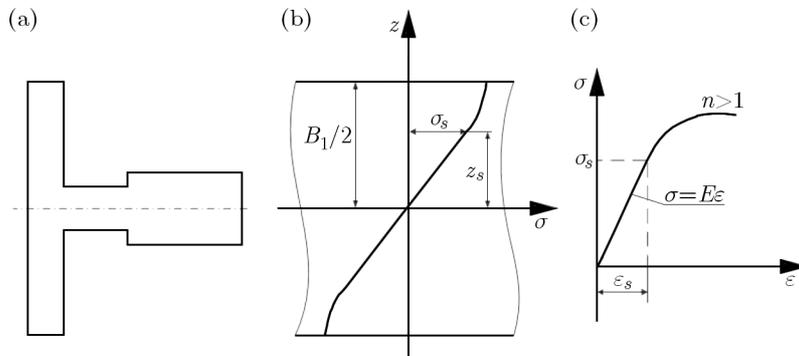
where $K' = K(\sigma_s/E)^n$.

Fig. 3. The stress distribution through the rail section: (a) stress distribution after bending, (b) residual stress distribution after springback, (c) stress-strain curve of elastic-plastic power-exponent hardening material

Then, for the force equilibrium across the section

$$M_x = 2\int\limits_0^{z_s} z\frac{z}{z_s}\sigma_s(H_1 - H_3)\,dz + 2\int\limits_0^{\frac{B_2}{2}} z\frac{z}{z_s}\sigma_s(H_3 + H_4)\,dz$$

$$+ 2\int\limits_0^{\frac{B_3}{2}} z\frac{z}{z_s}\sigma_s(H_2 - H_4)\,dz + 2\int\limits_{z_s}^{\frac{B_1}{2}} z\Big[\sigma_s\frac{z}{z_s} - K'\Big(\frac{z}{z_s} - 1\Big)^n\Big](H_1 - H_3)\,dz \tag{2.13}$$

Equations (2.13) and (2.2) reduce to the following equations

$$\frac{M_x}{M_t} = \frac{1}{\xi} - \frac{3B_1^3(H_1 - H_3)K'\xi^2\Big[\frac{\big(\frac{1}{\xi}-1\big)^{n+2}}{n+2} + \frac{\big(\frac{1}{\xi}-1\big)^{n+1}}{n+1}\Big]}{\sigma_s[(H_1 - H_3)B_1^3 + (H_3 + H_4)B_2^3 + (H_2 - H_4)B_3^3]} \tag{2.14}$$

Then, from equations (2.7), (2.8) and (2.14), the relation between C_Σ and x can be obtained $(2M_t/F \leqslant x \leqslant l)$

$$\frac{Fx}{2M_t} = \frac{C_\Sigma}{C_t} - \frac{3B_1^3(H_1 - H_3)K'\big(\frac{C_\Sigma}{C_t}\big)^{-2}\Big[\frac{\big(\frac{C_\Sigma}{C_t}-1\big)^{n+2}}{n+2} + \frac{\big(\frac{C_\Sigma}{C_t}-1\big)^{n+1}}{n+1}\Big]}{\sigma_s[(H_1 - H_3)B_1^3 + (H_3 + H_4)B_2^3 + (H_2 - H_4)B_3^3]} \tag{2.15}$$

So combining equations (2.10) and (2.15), the load-deflection curves can be plotted under the elastic-plastic power-exponent hardening model.

3. Experiments

To verify the load-deflection model, experiments are carried out respectively on the universal testing machine and the self-made hydraulic straightening machine. Take T/89 rail for test and the material considered for the rail is low carbon steel Q235 with following parameters: $E = 206000\,\text{MPa}$, $\sigma_s = 235\,\text{MPa}$; $K = 200000\,\text{MPa}$, $n = 1.02$, $\lambda = 0.0173$. And the rail section has dimensions of $H_1 = 20.9\,\text{mm}$, $H_2 = 41.1\,\text{mm}$, $H_3 = 11.3\,\text{mm}$, $H_4 = 7.7\,\text{mm}$, $B_1 = 89\,\text{mm}$, $B_2 = 10\,\text{mm}$, $B_3 = 15.88\,\text{mm}$.
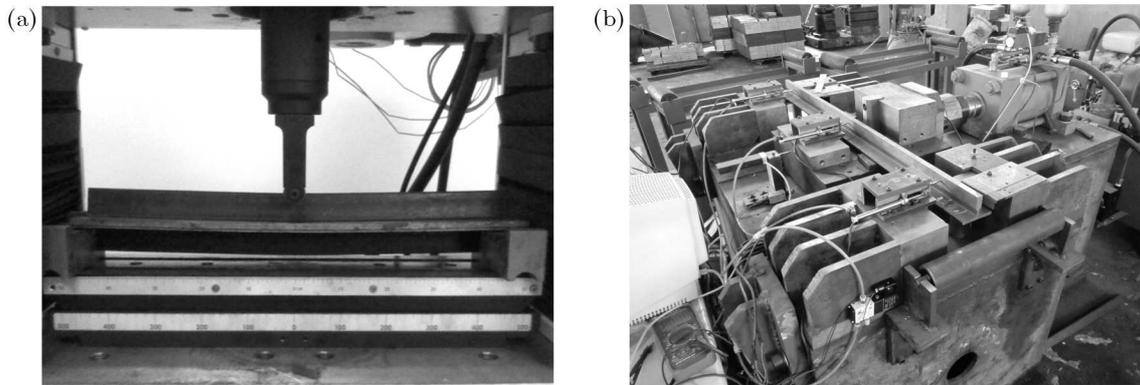
Fig. 4. Experimental set-up: (a) on the universal testing machine $(2l = 500\,\text{mm})$, (b) on the self-made hydraulic straightening machine $(2l = 1000\,\text{mm})$

Figure 4a shows the experimental set-up on the universal testing machine AG-1 introduced from Shima dzu Corporation. The rail is moment-free supported at both ends. And the distance

between the end supports is $500\,\mathrm{mm}$, that is $2l = 500\,\mathrm{mm}$. During the test, the loading part in the middle is moved at the speed of $0.1\,\mathrm{mm/s}$, providing the loading force. And the results of this test are shown in Fig. 5a.

Figure 4b shows the experimental set-up on the self-made hydraulic straightening machine. The rail is also moment-free supported at both ends. But the distance between the end supports is $1000\,\mathrm{mm}$, that is $2l = 1000\,\mathrm{mm}$. During the experiment, the loading part is moved at the speed of $0.6\,\mathrm{mm/s}$. The results are illustrated in Fig. 5b.
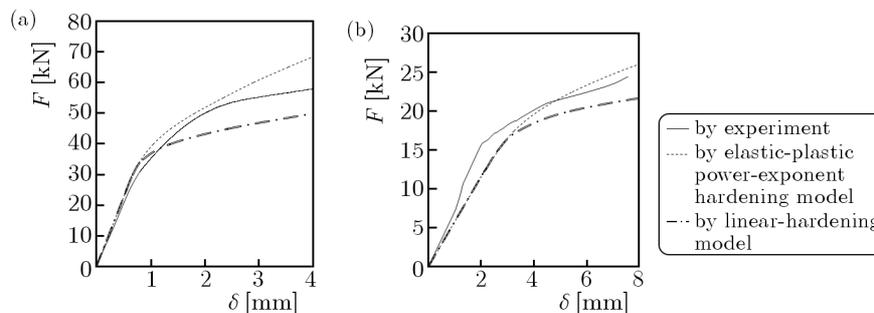

Fig. 5. Comparison of the results by experiment and model: (a) on the universal testing machine ($2l = 500\,\mathrm{mm}$), (b) on the self-made hydraulic straightening machine ($2l = 1000\,\mathrm{mm}$)

Figures 5a and 5b show the comparison of results by the experiment and by the model. It can be found that the load-deflection curves calculated with the elastic-plastic power-exponent hardening model are closer to the experimental results than those with the linear-hardening model.

As shown in Fig. 5a, the relative error of the results obtained with the elastic-plastic power-exponent hardening model will become larger with the increase of the loading stroke δ. So in the case of large elastic-plastic bending deformation, the real material hardening model is more complicated, and taking into account contact stresses and strains in the vicinity of the loading device is necessary to enhance the accuracy of the analytical results.

4.   Conclusions

In this paper, the load-deflection relations of T-section rails under lateral loads are studied based on elastic-plastic theory. The linear hardening model and the elastic-plastic power-exponent hardening model are used for the analysis. To verify the model, experiments are carried out respectively on a universal testing machine and a self-made hydraulic straightening machine. From the results presented in this paper, the followings are concluded:

- The load-deflection curves calculated with the elastic-plastic power-exponent hardening model are closer to the experimental results than those with the linear-hardening model.

- In the case of large elastic-plastic bending deformation, the real material hardening model is more complicated, and taking into account contact stresses and strains in the vicinity of the loading device is necessary to enhance the accuracy of the analytical results.

References

1. BIEMPICA C.B., DIAZ J.J.D., NIETO P.J.G., SANCHEZ I.P., 2009, Nonlinear analysis of residual stresses in a rail manufacturing process by FEM, *Advanced Mathematical Modeling*, **33**, 1, 34-53

2. CHUI PU, 1994, *Straightening Theory and Parameters Calculation*, Mechanical Industry Press, China

3. EGGERTSEN P.-A., MATTIASSON K., 2010, An efficient inverse approach for material hardening parameter identification from a three-point bending test, *Engineering with Computers*, **26**, 2, 159-170

4. JOHNSON W., YU T., 1981, On springback after the pure bending of beams and plates of elastic work-hardening materialsIII, *International Journal of Mechanical Sciences*, **23**, 10, 687-695

5. KATOH T., URATA E., 1993, Measurement and control of a straightening process for seamless pipes, *ASME J. Eng. Indus.*, **115**, 347-351

6. LI J., XIONG G., 2007, Study on calculation method of press straightening stroke based on straightening process model, *Key Engineering Materials*, **340-341**, 2, 1345-1350

7. LI J., ZOU H.J., XIONG G.L., 2004, Establishment and application of load-deflection model of press straightening, *Advances in Engineering Plasticity and its Applications*, **274**, 1/2, 475

8. MASMOUDI R., THERIAULT M., BENMOKRANE B., 1998, Flexural behavior of concrete beams reinforced with deformed fiber reinforced plastic reinforcing rods, *ACI Structural Journal*, **95**, 6, 665-676

9. OMERSPAHIC E., MATTIASSON K., ENQVIST B., 2006, Identification of material hardening parameters by the three-point bending of metal sheets, *International Journal of Mechanical Sciences*, **48**, 1525-1532

10. OU J.P., WANG B., HE Z., ZHANG X.Y., QIAN M.Z., 2004, Load-deflection response of concrete beams reinforced with FRP bars, *Advances in Structural Engineering*, **7**, 5, 427-436

11. SHEN H.B., SOKOLINSKY V.S., NUTT S.R., 2004, Accurate predictions of bending deflections for soft-core sandwich beams subject to concentrated loads, *Composite Structures*, **64**, 1, 115-122

12. SOKOLINSKY V.S., SHEN H., VAIKHANSKI L., NUTT S.R., 2003, Experimental and analytical study of nonlinear bending response of sandwich beams, *Composite Structures*, **60**, 2, 219-229

13. TSAI SHANG-HIS, KAN HENG-CHUAN, 2008, The exact solution of the load-deflection model of a uniformly loaded rectangular cross-section cantilever beam, *Journal of Physics D: Applied Physics*, **41**, 095502

14. TSAI SHANG-HIS, WANG YENG-TSENG, KAN HENG-CHUAN, 2009, Analysis on the uniformly loaded rectangular cross-section cantilever by a modified load-deflection model, *Journal of Physics D: Applied Physics*, **42**, 045505

15. VOLEBOV I.F, POLYAKOV A.P, KOLMOGOROV S.V., 1994, Mathematical model of rail straightening and experimental estimation of its adequacy, *Journal of Materials Processing Technology*, **40**, 1/2, 213-218

16. WU B.J., CHAN L.C., LEE T.C., ET AL., 2000, A study on the precision modeling of the bars produced in two cross-roll straightening, *Journal of Materials Processing Technology*, **99**, 202-206

Charakterystyki obciążeniowo-odkształceniowe szyn o przekroju teowym poddanych obciążeniom poprzecznym

Streszczenie

W pracy zaprezentowano charakterystyki obciążeniowo-odkształceniowe obciążanych poprzecznie szyn o przekroju teowym otrzymane na podstawie teorii lepkosprężystości. W badaniach przyjęto model materiału o liniowym oraz potęgowym umocnieniu. Podano analityczne wyrażenia dla krzywych obciążenia w funkcji odkształcenia. W wyniku weryfikacji eksperymentalnej stwierdzono, że charakterystyki obciążeniowo-odkształceniowe otrzymane przy zastosowaniu modelu z potęgowym umocnieniem materiału są bliższe rezultatom doświadczalnym niż w przypadku modelu z umocnieniem liniowym.